Electronic Supplementary Material (ESI) for Journal of Materials Chemistry A.

Electronic supplementary information

Prelithiated perfluoro-ionomer as an alternative binder for the state-of-the-art Ni-rich LiNi0.8Co0.15Al0.05O2 cathode of next-generation lithium-ion batteries

Selvamani Vadivel [a,b] and Montree Sawangphruk [a,b,*]

[a]Department of Chemical and Biomolecular Engineering, School of Energy Science and Engineering, Vidyasirimedhi Institute of Science and Technology, Rayong 21210, Thailand.

[b]Centre of Excellence for Energy Storage Technology (CEST), Vidyasirimedhi Institute of Science and Technology, Rayong 21210, Thailand.

Corresponding author: montree.s@vistec.ac.th (Montree Sawangphruk)

Table. S1. Crystallographic parameter obtained from the Rietveld refinement process for lithiated Nafion binder used NCA electrode (uncycled) prepared in ethanol (EBNCA) and NMP (NBNCA) dispersant.

	EBNCA	**NBNCA**
Space group/no.: R -3 m / 16 (Z : 3)	$a = b$ = 2.8678 (4) (Å) c = 14.1901 (3) (Å) V = 101.067 (3) $(Å)^3$ c/a = 4.94808	$a = b$ = 2.87035 (4) (Å) c = 14.1963 (3) (Å) V = 101.292 (3) $(Å)^3$ c/a = 4.9458
Wyckoff position 3a (0, 0, 1/2)		
Li (+)	0.9777	0.9758
Ni (2+) (exchanged)	0.02227	0.02399
Wyckoff position 3b (0, 0, 0)		
Li (+) (exchanged)	0.02227	0.02399
Ni (3+)	0.7777	0.7668
Co (3+)	0.1475	0.1503
Al (3+)	0.05	0.057
Wyckoff position 6c (0, 0, z)		
O	(z = 0.26614)	(z = 0.2608)
R_{Bragg}	1.967	1.492
χ^2	3.42	2.47

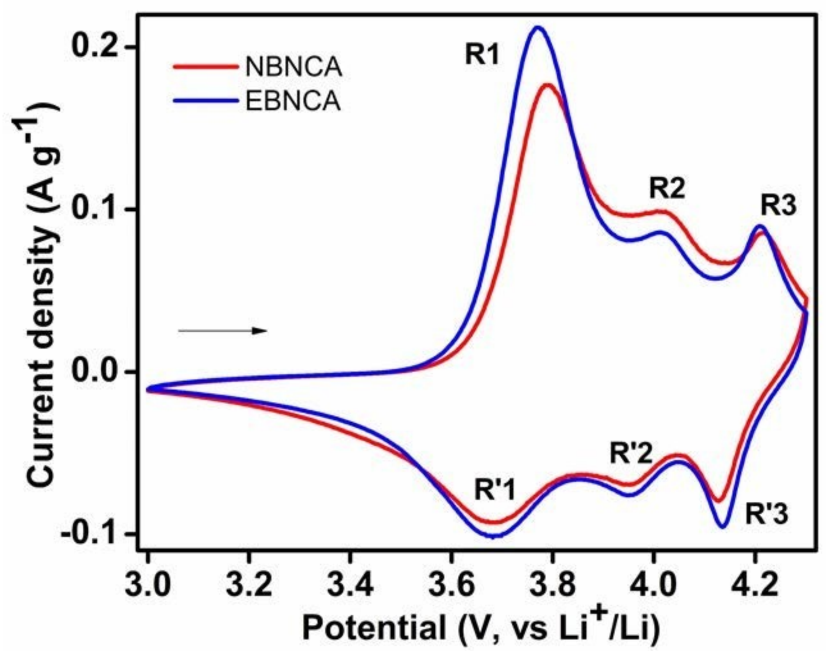

Fig. S1 Normalized CV curves recorded at a scan rate of 0.1 mV s^{-1} for the NCA electrode with lithiated Nafion binder in ethanol (EBNCA) and NMP medium (NBNCA).

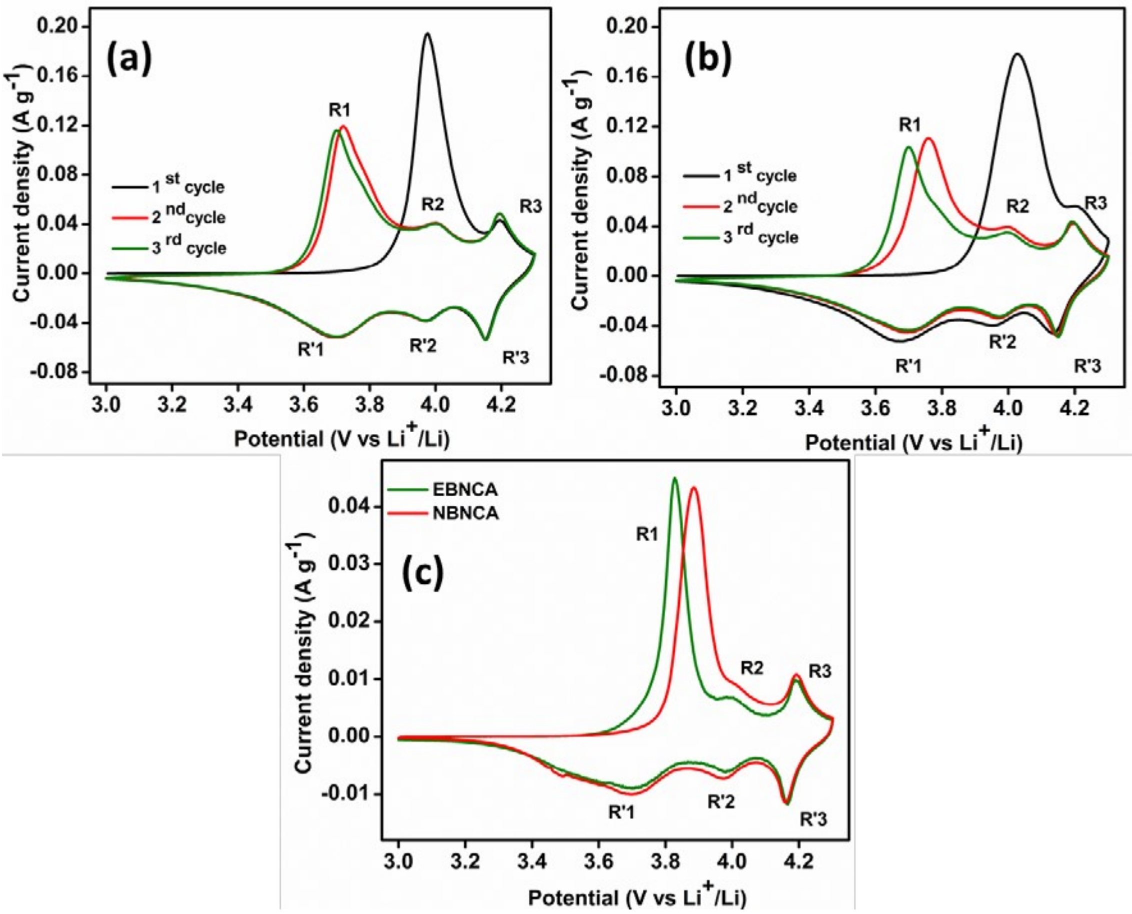

Fig. S2 Cyclic voltammogram recorded for the Li-Nafion binder used NCA cathode (a) and (b) EBNCA, and NBNCA cells at a scan rate of 0.05 mV s^{-1}, respectively and (c) Comparison of normalized CV recorded at a scan rate of 0.01 mV s^{-1}.

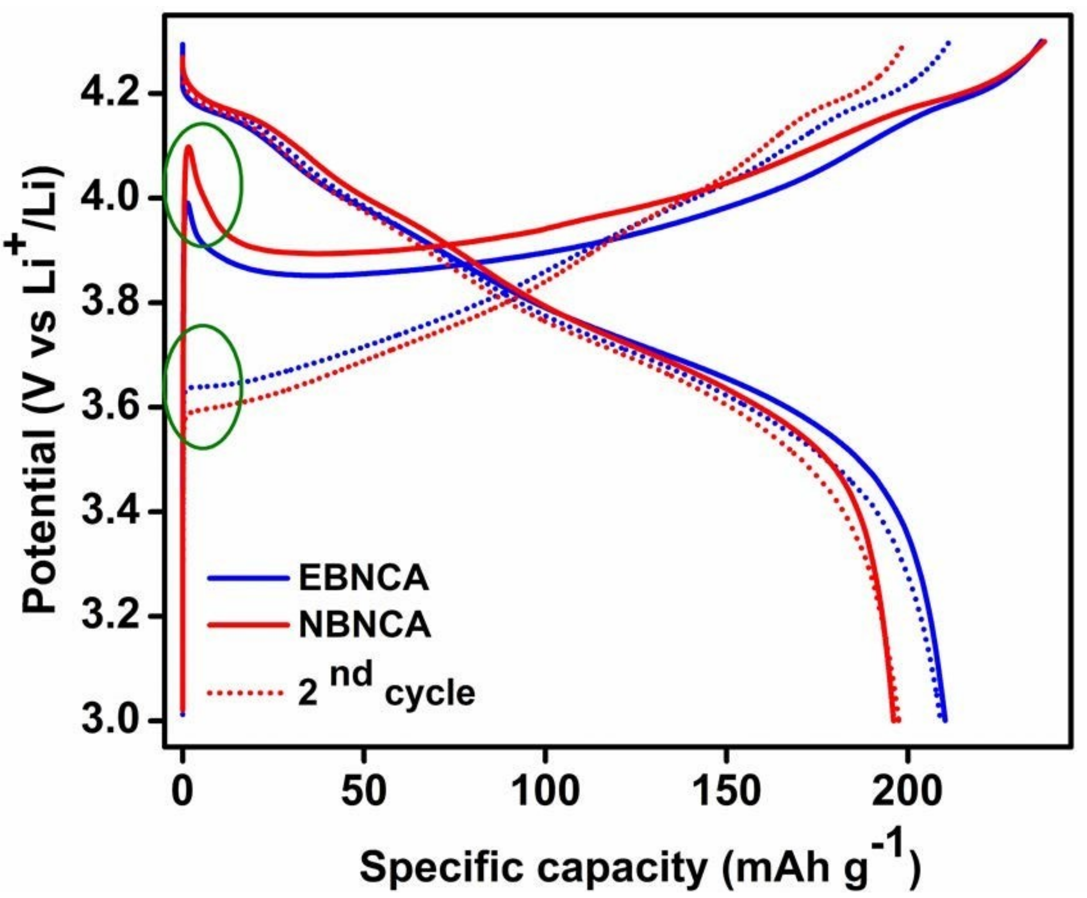

Fig. S3 First two consecutive cycles of NCA cathode with Li-Nafion binder in ethanol (EBNCA) and NMP medium (NBNCA) at a specific current of 0.1 C.

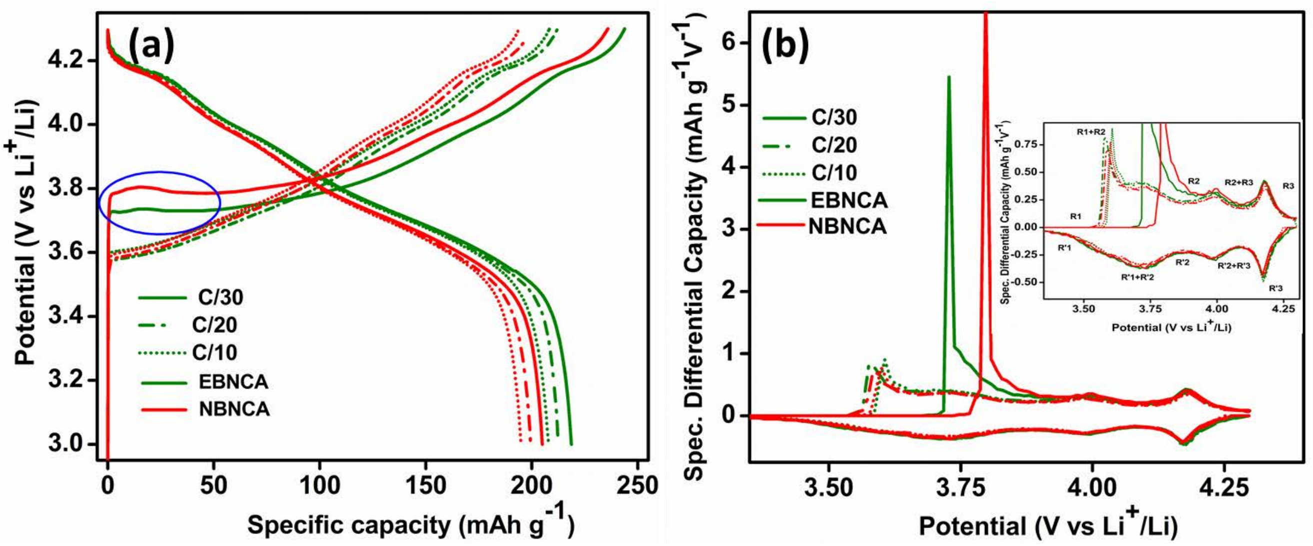

Fig. S4 (a) Comparison of galvanostatic charge/discharge profile and (b) Specific differential capacity plot as a function of voltage at different C-rates for EBNCA and NBNCA cells.

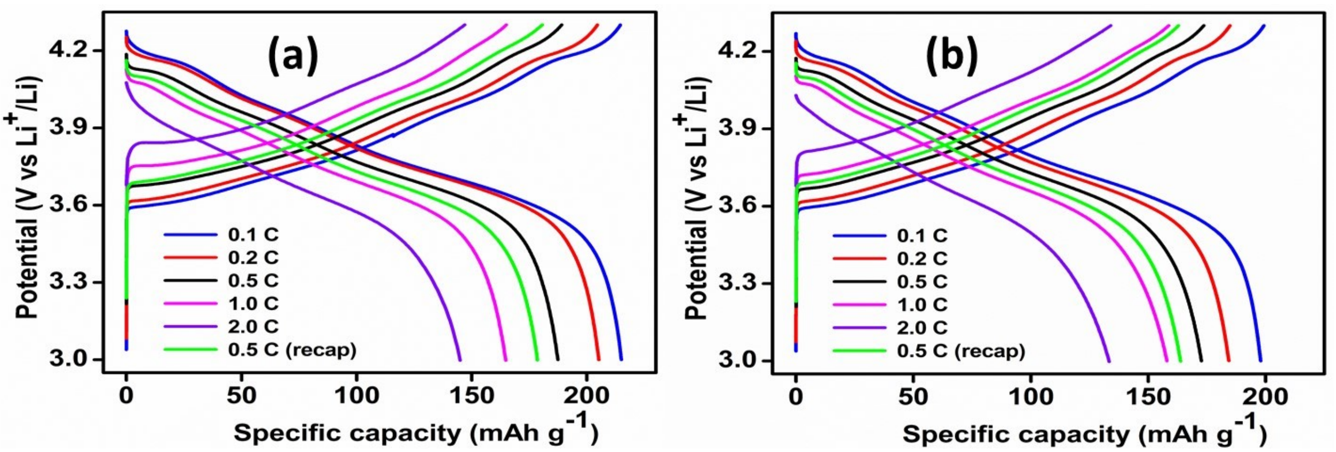

Fig. S5 Cycling profile obtained at different C rates (a) EBNCA and (b) NBNCA cells.

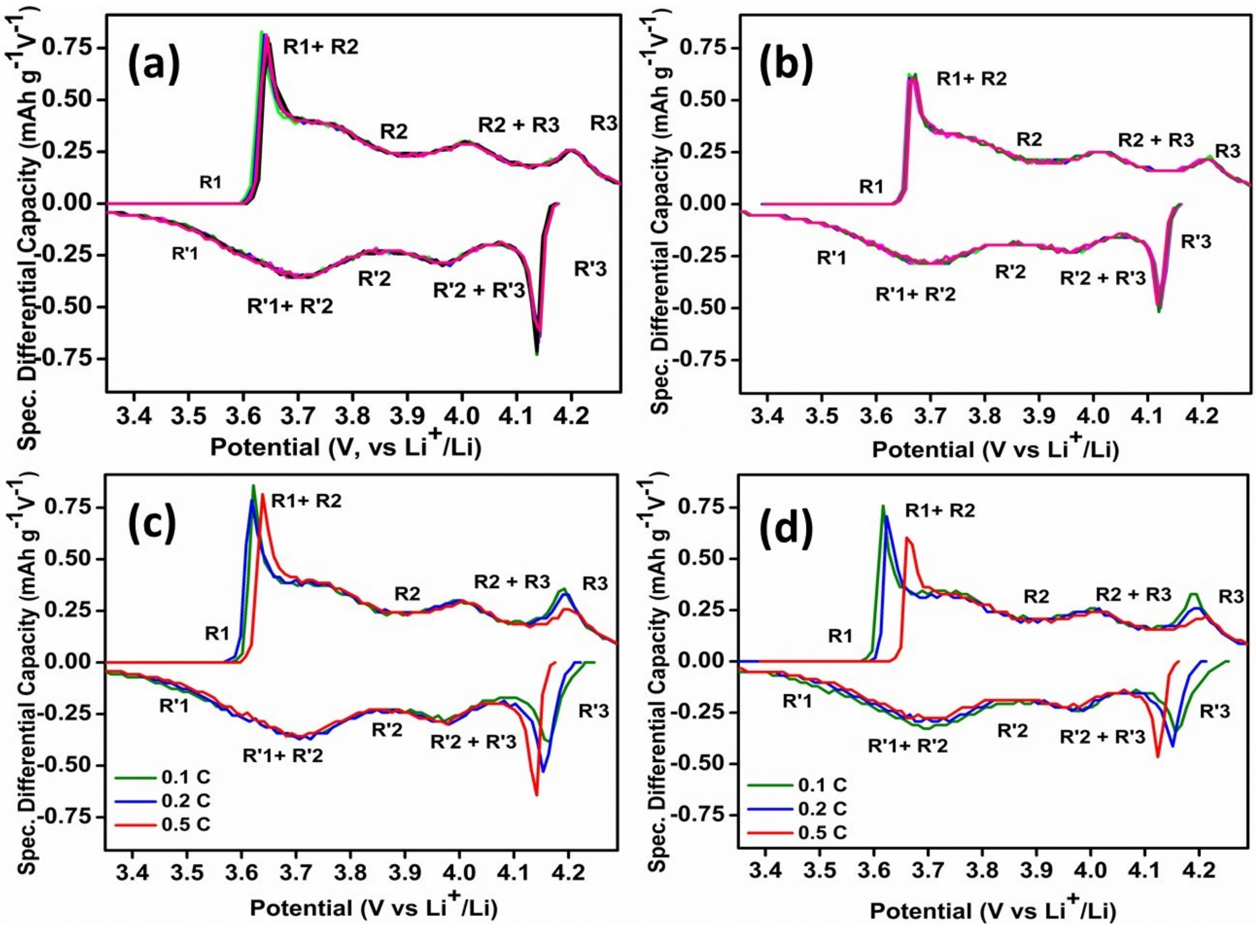

Fig. S6 Differential specific capacity as a function of voltage at a specific capacity of 0.5 C, and different C rates along with corresponding phase formation (a), (c) for EBNCA, and (b), (d) for NBNCA, respectively.

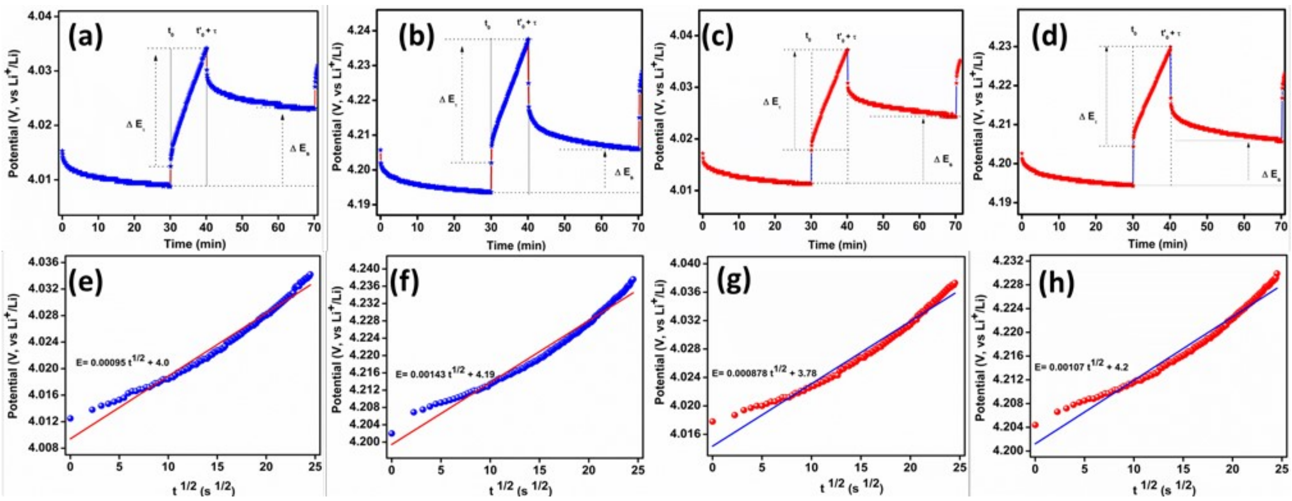

Fig. S7 Selected region of GITT curves recorded during the charging process (a) - (d) Voltage change as a function of time during the positive pulse current and (e) - (h) Linear fitted V vs $t^{1/2}$ plot. ((a),(b) & (e), (f) for EBNCA cell and (c), (d) & (g), (h) for NBNCA cell).

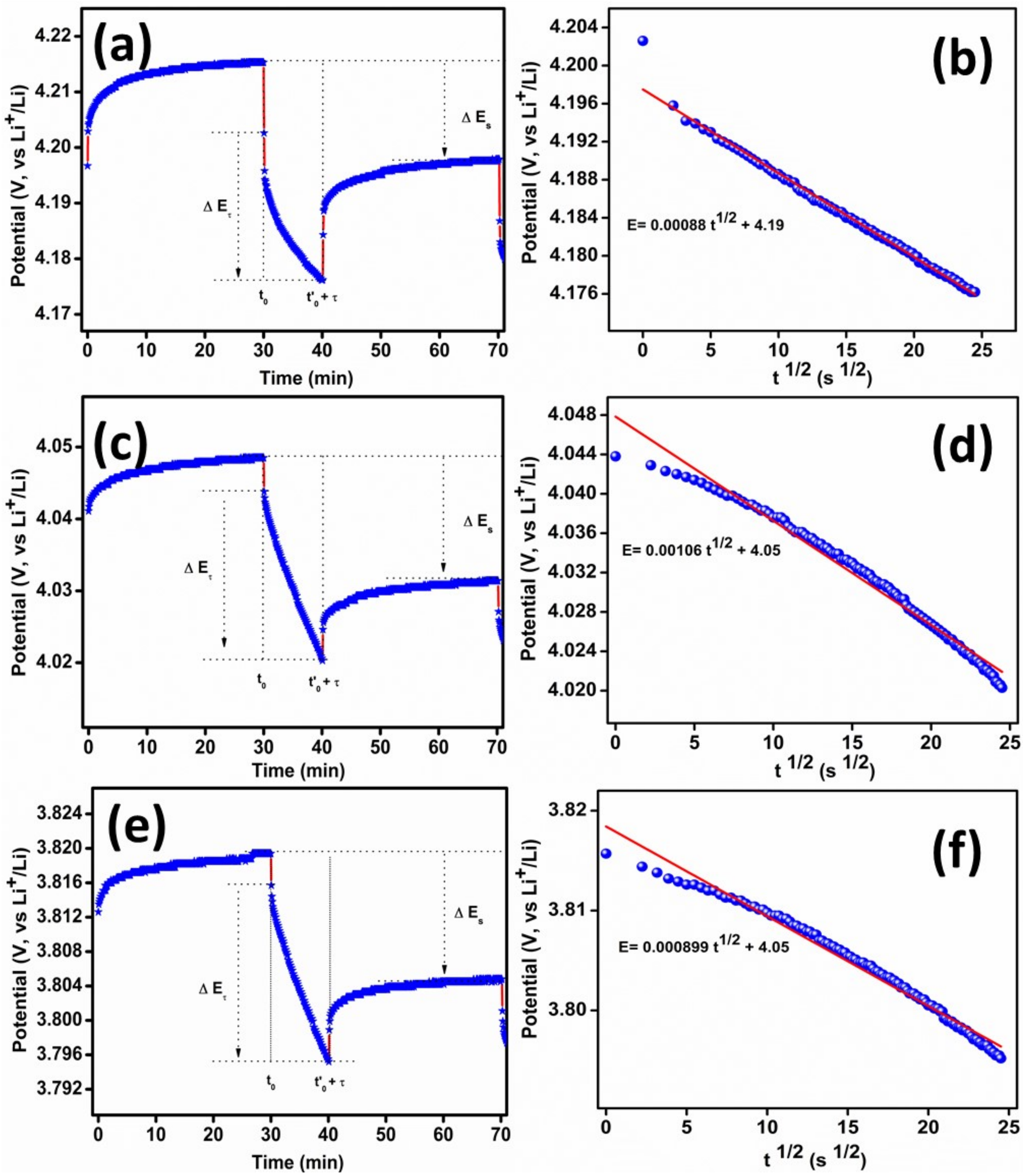

Fig. S8 The selected region of GITT titration curve for EBNCA cell obtained during the negative pulse current (a), (c), (e) Steady voltage change vs time and (b), (d), (f) Linear relationship between V and $t_{1/2}$.

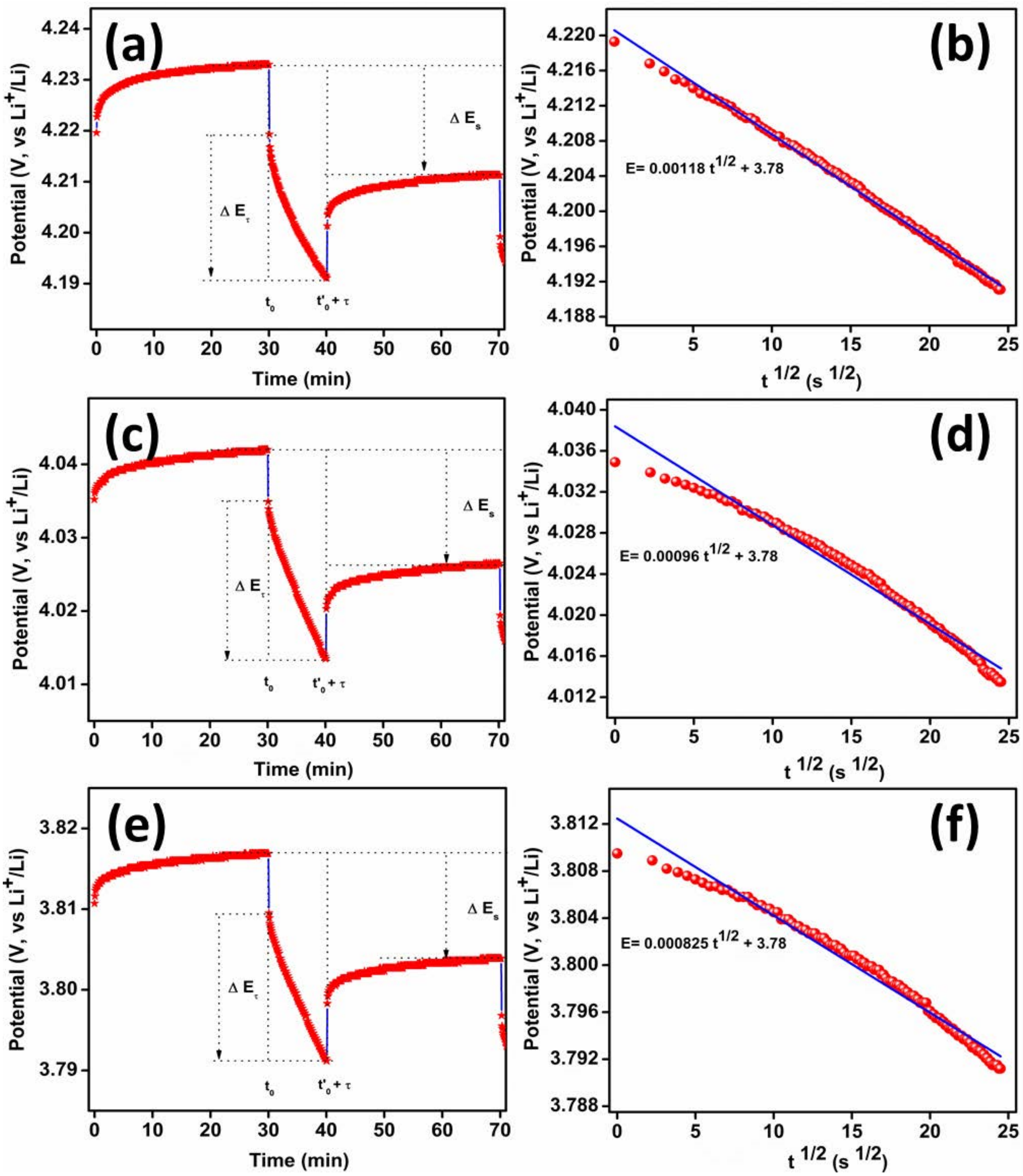

Fig. S9 The selected region of GITT titration curve for NBNCA cell obtained during the negative pulse current (a), (c), (e) Steady voltage change vs time and (b), (d), (f) Linear relationship between V and $t_{1/2}$.

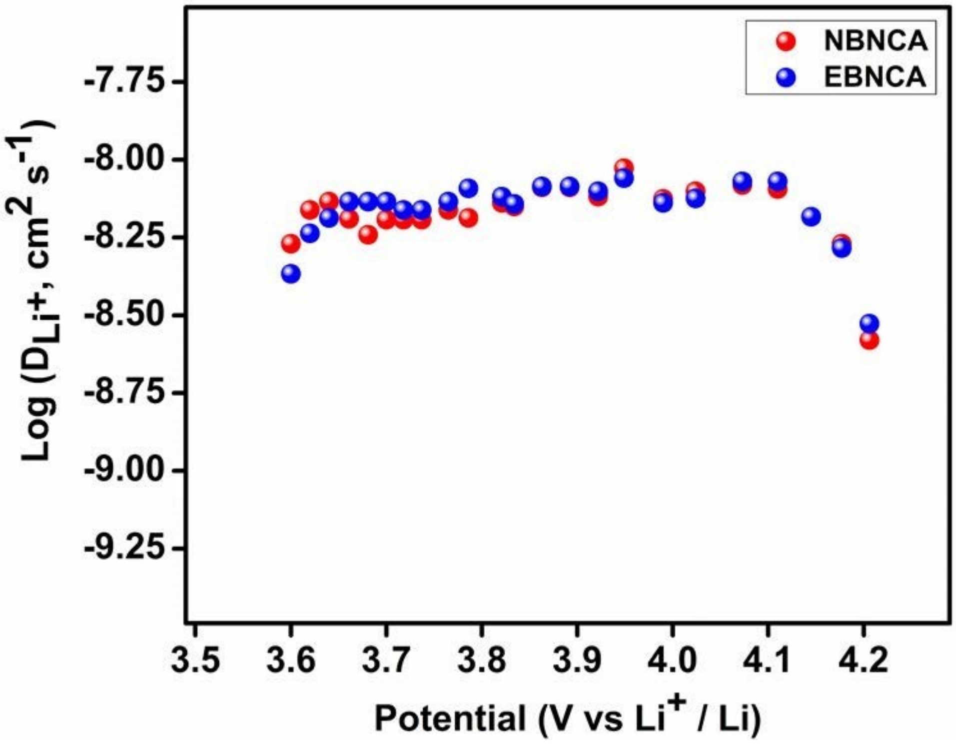

Fig. S10 The calculated chemical lithium diffusion coefficient as a function of cell voltage at a constant pulse of 0.1 C during the charging process.

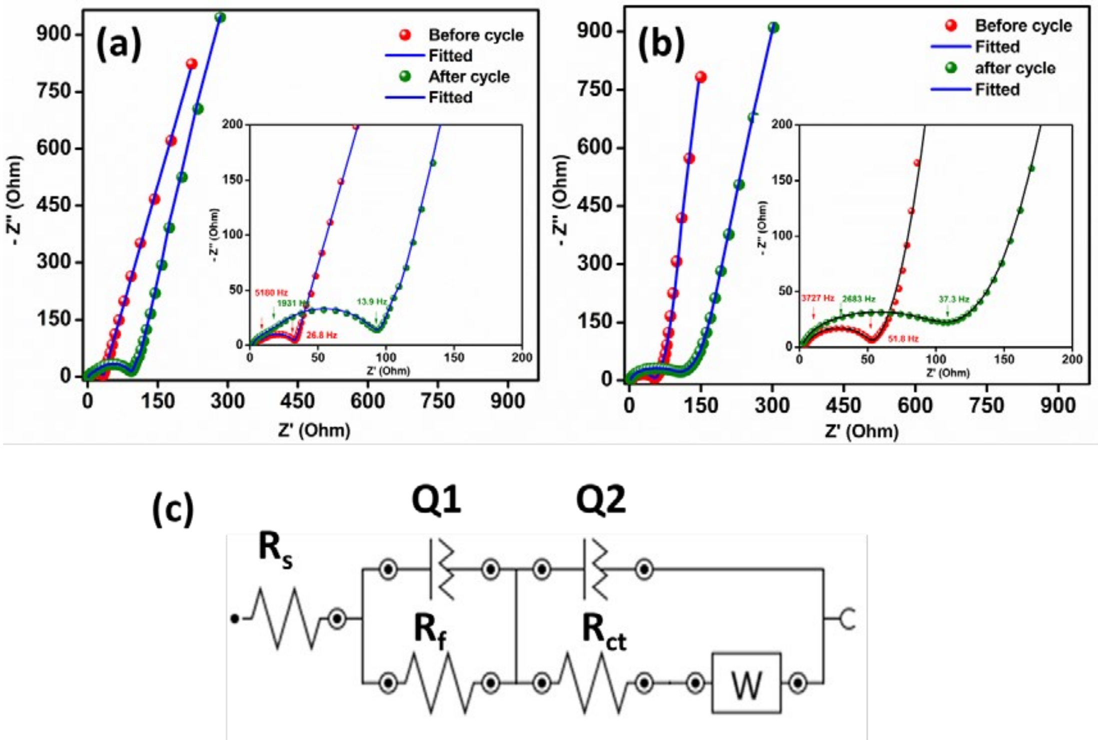

Fig. S11 EIS spectra of before and after cycling (a) EBNCA, (b) NBNCA cell, and (c) Randle's equivalent circuit generated by the fitting software. (inset: high magnifications).

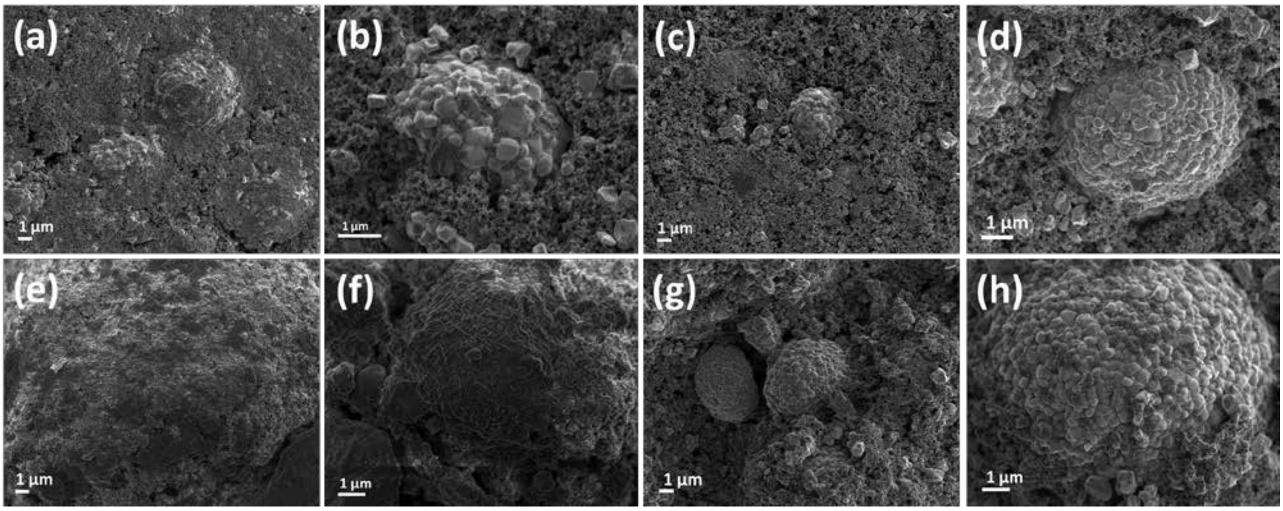

Fig. S12 FE-SEM images of (a) - (d) uncycled electrodes, and (e) – (h) cycled electrodes after the lifecycle test. (a),(b) & (e), (f) represents EBNCA and (c), (d) & (g), (h) denotes NBNCA, where (b), (d), (f) and (h) are high magnified images.

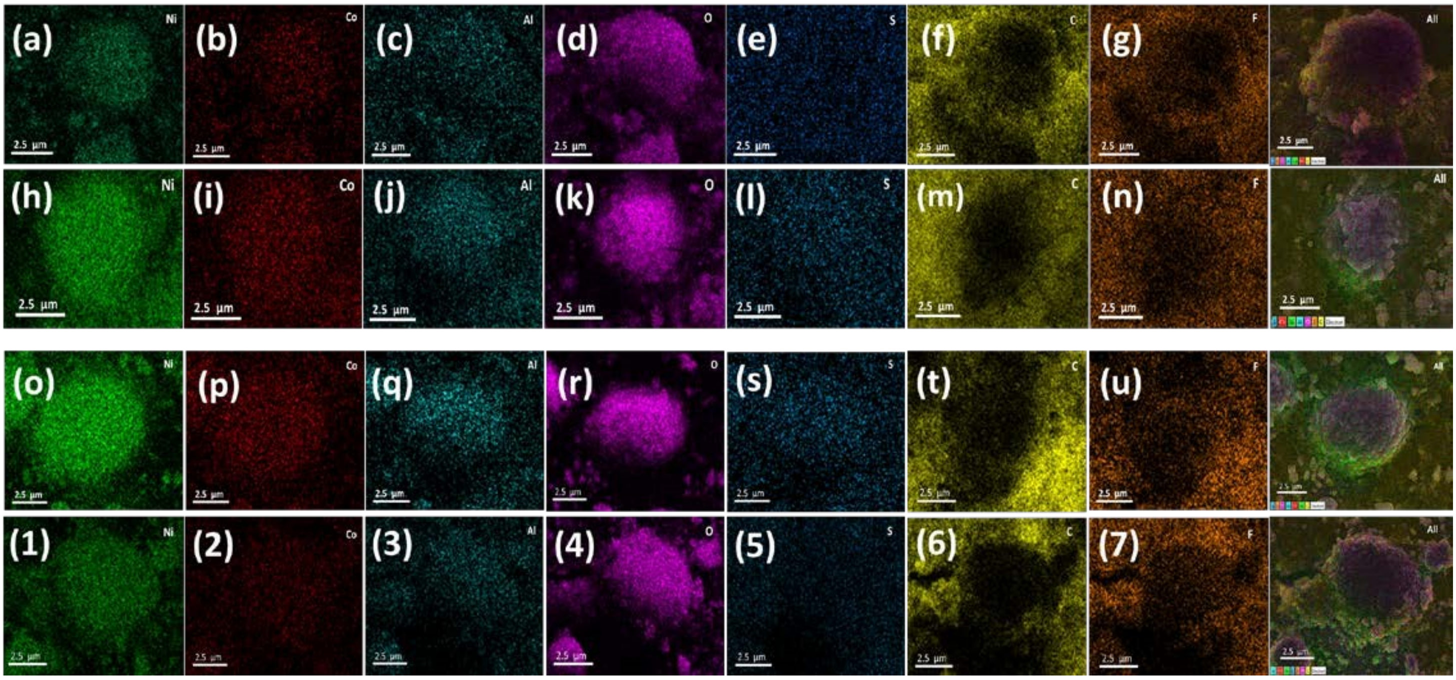

Fig. S13 Energy dispersive X-ray analysis (EDX) mapping of before and after life-cycled electrodes. (a) – (g) Uncycled EBNCA, (h) – (n) Cycled EBNCA electrode, (o) – (u) uncycled NBNCA, and (1) – (7) cycled NBNCA electrodes.

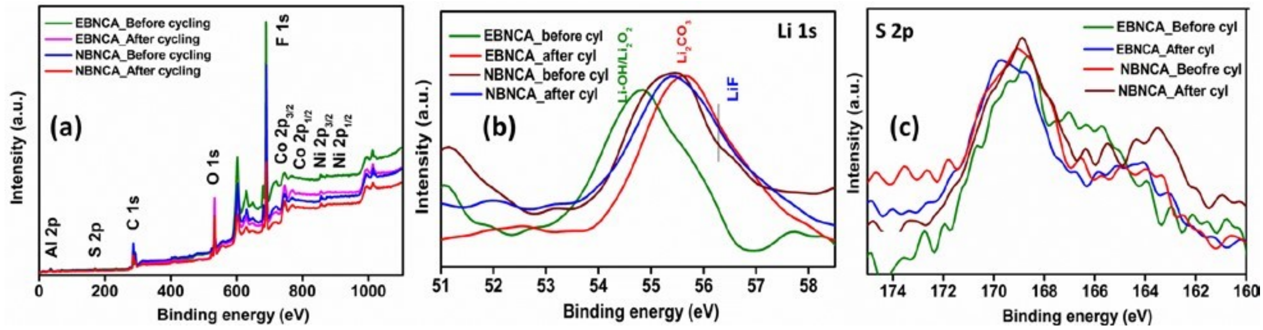

Fig. S14 Compiled spectra of (a) Wide scan, (b) Li 1s and (c) S 2p atoms.

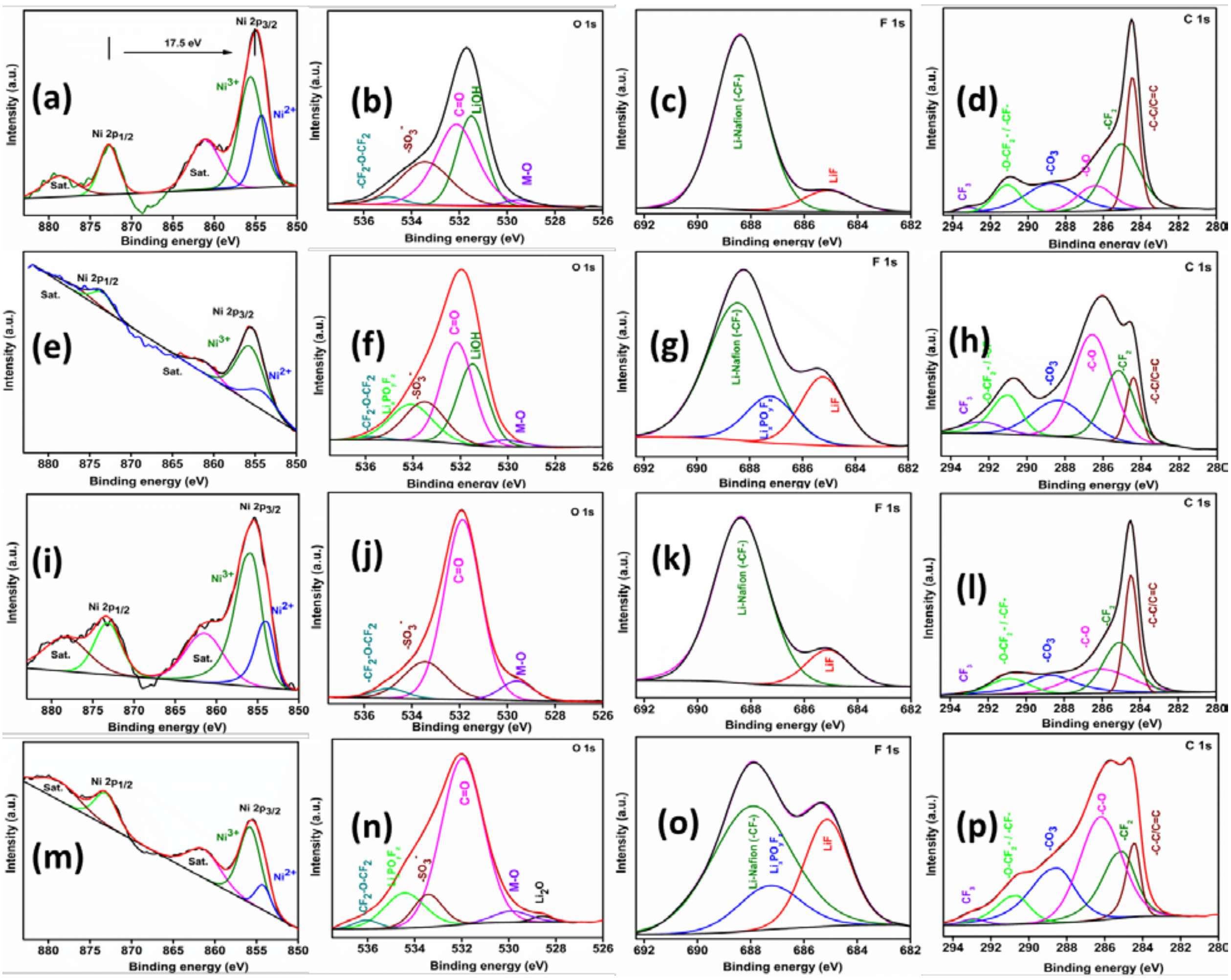

Fig. S15 Deconvoluted XPS spectra of Ni 2p, O 1s, F 1s and C 1s orbital of uncycled (a-d, EBNCA & i-l, NBNCA) and cycled (e-h, EBNCA & m-p, NBNCA) electrodes.

Percentage of Li present in the lithiated-Nafion calculated from the ICP

Procedure: 0.5 ml of the lithiated polymer solution (stock in ethanol) was dried under reduced pressure. The dried mass was digested with concentrated nitric acid + H_2O_2 mixture and further diluted for ICP measurements.

The dried lithiated-polymer weight is 38.8 mg and initially digested under strong acidic-oxidizing medium followed by diluted to 1.0 L (ie. 38.8 ppm)

Note: The labile or exchangeable lithium-ion has been replaced with H^+.

Hence,

38.8 ppm solution contains (polymer + lithium $_{(solubilized)}$)

The stock solution (about 2.57 ml) was further diluted to 100 ml

The concentration of lithium present in the unknown solution was found to be 0.013 ppm

From the back-calculation, it is found to be 0.506 ppm of lithium present in the bulk solution.

Ie. 38.8 ppm contains 0.506 ppm of lithium and 38.294 ppm of Nafion polymer, which corresponds to 1.3 percentage of lithiation.

Similarly,

The effect of ethanol wash has also been investigated, especially for lithium, by employing ICP-OES analysis and compared with the pristine material, regardless of composition. (note: for this study new bulk batch material has been collected, which contains slightly more Ni)

Herein, 0.25 ppm of the stock solution has been prepared, which contains 0.0252 ppm of lithium, whereas the ethanol washed sample displays the final concentration of about 0.0225 ppm. The above result further supports the existence of Li-OH residue in the present sample.

Table S2 Lithium concentration obtained from ICP-OES.

Sample	**Element**	**Molecular weight (mg/mole)**	**λ (nm)**	**R^2**	**Concentration (ppm)**
P-NCA	Li	6941.00	670.763	0.999816	0.025200000
NCA-washed	Li	6941.00	670.763	0.999816	0.022500000
Li-Nafion	Li	6941.00	670.763	0.999816	0.01300

Table S3. Comparison of electrochemical performance of NCA materials with different binders.

S.No	Material	Specific discharge capacity (mAh g^{-1})	Rate (C)	Remarks
1	**NCA with lithiated Nafion In Ethanol medium**	**166** (1C= 200 mAh g^{-1})	**1.0**	**Present study**
		141	**2.0**	
	In NMP medium	**155**	**1.0**	
		134	**2.0**	
2	NCA with PVDF	**146** (1C= 200 mAh g^{-1})	1.0	**[1]**
		131	2.0	
3	NCA with PVDF	163 (1C= 180 mAh g^{-1})	1.0	[2]
		154	2.0	
4	Carbon coated NCA with PVDF	140	1.0	[3]
		83	3.0	
5	EDTA modified NCA with PVDF	170 (1C= 180 mAh g^{-1})	1.0	[4]
		160	2.0	
	Pristine NCA with PVDF	150	1.0	
		125	2.0	
6	Na doped NCA Un doped NCA with PVDF	149	2.0	[5]
		140		
7	LBO coated NCA with PVDF	153	2.0	[6]
	Pristine NCA	145		
8	Li_2TiO_3 coated NCA with PVDF binder	160 (1C= 180 mAh g^{-1})	1.0	[7]
		150	2.0	

Table. S4 Comparison of diffusion coefficient for Ni-rich cathodes.

S.No	Electrode Materials	Binder type	Diffusion coefficient (D_{Li+}) (cm^2 s^{-1})	Method employed	Reference
1	**$LiNi_{0.8}Co_{0.15}Al_{0.05}O_2$**	**Pre-lithiated Nafion**			**Present work**
		Ethanol	**7.68×10^{-9}**	**GITT**	
			5.69×10^{-9}	**CV**	
		NMP	**6.34×10^{-9}**	**GITT**	
			5.04×10^{-9}	**CV**	
2.	$LiNi_{0.8}Co_{0.15}Al_{0.05}O_2$ (Coated with spinel $LiNi_{0.5}Mn_{1.5}O_4$)	PVDF	1.38×10^{-10}	GITT	[8]
	$LiNi_{0.8}Co_{0.15}Al_{0.05}O_2$ (pristine)		1.03×10^{-10}		
3.	$LiNi_{0.9}Co_{0.07}Al_{0.03}O_2$ (doped with Al)	PVDF	2.39×10^{-9}	EIS	[9]
	$LiNi_{0.9}Co_{0.07}Al_{0.03}O_2$ (coated with $LiAlO_2$)		8.08×10^{-9}		
4.	$LiNi_{0.815}Co_{0.15}Al_{0.035}O_2$	PVDF	5.57×10^{-10}	CV	[10]
5.	$LiNi_{0.8}Co_{0.15}Al_{0.05}O_2$	PVDF	1.45×10^{-10}	CV	[11]
6.	$LiNi_{0.8}Co_{0.1}Mn_{0.1}O_2$	PVDF	10^{-8} to 10^{-9}	GITT	[12]
7.	$LiNi_{0.7}Co_{0.15}Mn_{0.15}O_2$	PVDF	3.02×10^{-11}	CV	[13]
8.	$LiNi_{0.6}Mn_{0.2}Co_{0.2}O_2$	PVDF	$1 - 10 \times 10^{-11}$	GITT	[14]
9.	$LiNi_{0.6}Mn_{0.2}Co_{0.2}O_2$ (cold laser ablated)	PVDF	$1.6 – 5.3 \times 10^{-12}$ - 10^{-13}	CV	[15]

References

[1] Vadivel, S.; Phattharasupakun, N.; Wutthiprom, J.; Duangdangchote, S.; Sawangphruk, M. HighPerformance Li-Ion Batteries Using Nickel-Rich Lithium Nickel Cobalt Aluminium Oxide–Nanocarbon Core-Shell Cathode: In Operando X-Ray Diffraction. *ACS Appl. Mater. Interfaces* **2019**, *11* (34), 30719–30727. https://doi.org/10.1021/acsami.9b06553.

[2] Liu, B. S.; Wang, Z. B.; Yu, F. Da; Xue, Y.; Wang, G. J.; Zhang, Y.; Zhou, Y. X. Facile Strategy of NCA Cation Mixing Regulation and Its Effect on Electrochemical Performance. *RSC Adv.* **2016**, *6* (110), 108558–108565. https://doi.org/10.1039/c6ra20146f.

[3] Zhang, N.; Zhang, X.; Shi, E.; Zhao, S.; Jiang, K.; Wang, D.; Wang, P.; Guo, S.; He, P.; Zhou, H. In Situ X-Ray Diffraction and Thermal Analysis of LiNi0.8Co0.15Al0.05O2 Synthesized via Co-Precipitation Method. *J. Energy Chem.* **2018**, *27* (6), 1655–1660. https://doi.org/10.1016/j.jechem.2018.06.007.

[4] Wang, Y.; Sun, Y.; Liu, S.; Li, G.; Gao, X.-P. Na-Doped LiNi 0.8 Co 0.15 Al 0.05 O 2 with Excellent Stability of Both Capacity and Potential as Cathode Materials for Li-Ion Batteries. *ACS Appl. Energy Mater.* **2018**, *1* (8), 3881–3889. https://doi.org/10.1021/acsaem.8b00630.

[5] Chung, Y.; Ryu, S.-H.; Ju, J.-H.; Bak, Y.-R.; Hwang, M.-J.; Kim, K.-W.; Cho, K.-K.; Ryu, K.-S. A Surfactant-Based Method for Carbon Coating of LiNi 0.8 Co 0.15 Al 0.05 O 2 Cathode in Li-Ion Batteries. *Bull. Korean Chem. Soc.* **2010**, *31* (8), 2304–2308. https://doi.org/10.5012/bkcs.2010.31.8.2304.

[6] Qi, Huan; Guo, Wenxun; Tian, Lingyun; Wen, Xiaofeng; Shi, Kaiyue; Zheng, J. Facile Fabrication and Low-Cost Coating of LiNi0.8Co0.15Al0.05O2 with Enhanced Electrochemical Performance as Cathode Materials for Lithium-Ion Batteries. *Int. J. Electrochem. Sci.* **2017**, *12* (7), 5836–5844. https://doi.org/10.20964/2017.07.01.

[7] Wu, N.; Wu, H.; Liu, H.; Zhang, Y. Solvothermal Coating LiNi0.8Co0.15Al0.05O2 Microspheres with Nanoscale Li2TiO3 Shell for Long Lifespan Li-Ion Battery Cathode Materials. *J. Alloys Compd.* **2016**, *665*, 48–56. https://doi.org/10.1016/j.jallcom.2016.01.044.

[8] Y. Huang, X. Zhang, R. Yu, S. Jamil, S. Cao, S. Fang, Y. Wang, K. Tang, G. Chen, Z. Luo, X. Yang, X. Wang, Preparation and Performance of the Heterostructured Material with a Ni-Rich Layered Oxide Core and a LiNi 0.5 Mn 1.5 O 4 -like Spinel Shell, ACS Appl. Mater. Interfaces. 11 (2019) 16556–16566. https://doi.org/10.1021/acsami.9b01957.

[9] J. Duan, P. Dong, D. Wang, X. Li, Z. Xiao, Y. Zhang, G. Hu, A facile structure design of LiNi0.90Co0.07Al0.03O2 as advanced cathode materials for lithium-ion batteries via carbonation decomposition of NaAl(OH)4 solution, J. Alloys Compd. 739 (2018) 335–344. https://doi.org/10.1016/j.jallcom.2017.12.236.

[10] A. Hou, Y. Liu, L. Ma, F. Chai, P. Zhang, Y. Fan, High-rate LiNi0.815Co0.15Al0.035O2 cathode material prepared by spray drying method for Li-ion batteries, J. Mater. Sci. Mater. Electron. 31 (2020) 1159–1167. https://doi.org/10.1007/s10854-019-02627-9.

[11] Z. Tang, S. Wang, J. Liao, S. Wang, X. He, B. Pan, H. He, C. Chen, Facilitating Lithium-Ion Diffusion in Layered Cathode Materials by Introducing Li + /Ni 2+ Antisite Defects for High-Rate Li-Ion Batteries, Research. 2019 (2019) 1–10. https://doi.org/10.34133/2019/2198906.

[12] C. Hong, Q. Leng, J. Zhu, S. Zheng, H. He, Y. Li, R. Liu, J. Wan, Y. Yang, Revealing the correlation between structural evolution and Li + diffusion kinetics of nickel-rich cathode materials in Liion batteries, J. Mater. Chem. A. 8 (2020) 8540–8547. https://doi.org/10.1039/D0TA00555J.

[13] J. Tian, Y. Su, F. Wu, S. Xu, F. Chen, R. Chen, Q. Li, J. Li, F. Sun, S. Chen, High-Rate and CyclingStable Nickel-Rich Cathode Materials with Enhanced Li + Diffusion Pathway, ACS Appl. Mater. Interfaces. 8 (2016) 582–587. https://doi.org/10.1021/acsami.5b09641.

[14] S. Cui, Y. Wei, T. Liu, W. Deng, Z. Hu, Y. Su, H. Li, M. Li, H. Guo, Y. Duan, W. Wang, M. Rao, J. Zheng, X. Wang, F. Pan, Optimized Temperature Effect of Li-Ion Diffusion with Layer Distance in Li(Ni x Mn y Co z)O 2 Cathode Materials for High-Performance Li-Ion Battery, Adv. Energy Mater. 6 (2016) 1501309. https://doi.org/10.1002/aenm.201501309.

[15] P. Zhu, H.J. Seifert, W. Pfleging, The Ultrafast Laser Ablation of Li(Ni0.6Mn0.2Co0.2)O2 Electrodes with High Mass Loading, Appl. Sci. 9 (2019) 4067 (2–15). https://doi.org/10.3390/app9194067.